Pure & Appl. Chem., Vol. 63, No. 10, pp. 1473–1482, 1991.
Printed in Great Britain.

High frequency permittivity and its use in the investigation of solution properties

J. Barthel and R. Buchner

Institut für Physikalische und Theoretische Chemie der Universität Regensburg, D-8400 Regensburg, Germany

Abstract - Recent results from permittivity measurements at microwave to far-infrared frequencies are reported for various liquid electrolyte and non-electrolyte systems. They enlarge our knowledge on processes which produce (by their complex interplay of orientational, intramolecular, kinetic, H-bonding, diffusional and migrational modes) the properties of pure solvents, solvent mixtures and solutions.

Protic solvents show three relaxational processes: re-establishment of the perturbed solvent structure, "intramolecular" rotation of solvent molecules as monomers and in H-bonded chains or networks, and very short relaxation times of about 1 ps due to H-bond dynamics. Aprotic solvents display a more or less continuous relaxation time distribution. Solvent mixtures show a particular behaviour related to the properties of their constituents. The addition of salt affects the relaxation times of the solvents, but no new modes are generated by free ions. In contrast, ion pairs and other solute complexes act as dipoles and display specific relaxation processes.

Information from high frequency permittivity measurements is used to explanation and calculation of solution properties required by fundamental and applied research.

INTRODUCTION

The application of an electric field $\vec{E}$ ($\vec{E}$, electric field strength) to a liquid yields the polarization $\vec{P}$ of the liquid (eq.(1a)) consisting of two parts, $\vec{P}_\mu$ and $\vec{P}_\alpha$ (eqs.(1b,c)), separable by measurement. The time-dependent orientational polarization $\vec{P}_\mu$ is the result of the alignment of dipole molecules by the local electric field against thermal motion. The induced polarization $\vec{P}_\alpha$ is an intramolecular effect due to the action of the internal field on molecular polarizability, following changes of the electric field without delay up to far-infrared frequencies. $\vec{P}_\mu$ and $\vec{P}_\alpha$ are linearly independent. Their separation is achieved by the introduction of the so-called "infinite frequency permittivity" ε_∞ to which only $\vec{P}_\alpha$ contributes.

$$\vec{P} = \varepsilon_o(\varepsilon - 1)\vec{E}; \quad \vec{P}_\mu = \varepsilon_o(\varepsilon - \varepsilon_\infty)\vec{E}; \quad \vec{P}_\alpha = \varepsilon_o(\varepsilon_\infty - 1)\vec{E} \qquad (1a,b,c)$$

In eqs.(1) ε_o is the permittivity of the vacuum, ε is the relative permittivity of the liquid.

FREQUENCY DEPENDENCE OF PERMITTIVITY

With increasing frequency of an electromagnetic wave passing through a dielectric, situations are reached in which the polarity change of the electric field causes significant variation of the field strength within periods that are characteristic of molecular motions, such as dipole reorientation, ionic mobility, etc. Then polarization lags behind the electric field and energy is dissipated in the system. Energy dissipation is commonly treated with the help of complex numbers for the electric and magnetic field vectors ($\vec{E}$, $\vec{D}$, $\vec{H}$, $\vec{B}$) and for the physical properties permittivity, permeability and conductivity of the sample.

Figure 1a shows the idealized frequency dependence of the real part ε' of the complex permittivity $\hat{\varepsilon}(\omega)$, the dispersion curve; Figure 1b shows the corresponding imaginary part ε'', the absorption (loss) curve characterizing the energy loss. The decrease of ε' from static permittivity to ε_∞, accompanied by a broad absorption band in the ε'' diagram is characteristic for the reorganization of the liquid structure. This relaxation process reduces $\vec{P}_\mu$ from its static value to zero. The processes in the IR and UV region, affecting $\vec{P}_\alpha$ are resonant transitions.

Appropriate combination of the Maxwell equations yields the wave equation for a travelling

wave of circular frequency ω($\omega=2\pi\nu$, ν=linear frequency) in a medium of complex permittivity $\hat{\varepsilon}(\omega)$, permeability $\hat{\mu}(\omega)$ and conductivity $\hat{\kappa}(\omega)$

$$\nabla^2\vec{A} + \hat{k}^2\vec{A} = 0 \tag{2}$$

where $\vec{A}$ is either the electric field strength $\vec{E}$ or the magnetic field strength $\vec{H}$, both of which propagate in the medium with equal propagation coefficients

$$\hat{k}^2 = k_o^2\,\hat{\mu}(\omega)\,\hat{\eta}(\omega)\,; \quad k_o^2 = \varepsilon_o\mu_o\omega^2 = \left(\frac{\omega}{c_o}\right)^2 \tag{3a,b}$$

k_o and c_o are the propagation coefficient and the speed of light in vacuum. For the investigated electrolyte solutions and their solvents, the relative complex permeability $\hat{\mu}(\omega)$ equals unity. The quantity

$$\hat{\eta}(\omega) = \hat{\varepsilon}(\omega) - i\,\frac{\hat{\kappa}(\omega)}{\omega\varepsilon_o} \tag{4}$$

called the generalized permittivity of the sample [1] is - in the strictest acceptance of the Maxwell equations - the only measurable quantity for electrically conducting systems. For non-conducting systems ($\hat{\kappa}=0$), it is reduced to the complex permittivity $\hat{\varepsilon}(\omega)$. It is known from experiments that the frequency dependence of conductance is very small (Debye-Falkenhagen effect). For lack of better information, it is neglected at high frequencies, and generally the assumption is made that $\kappa''(\omega)=0$, $\kappa'(\omega)=\kappa'(0)=\kappa$; κ is the specific conductance at quasi-static (very low) frequencies of the investigated electrolyte solution

$$\kappa = \frac{N_A e}{1000}\sum_k c_k\,|z_k|\,u_k \tag{5}$$

composed of ions of charge ez_k and ionic mobility u_k at molarity c_k. Then it follows that

$$\hat{\eta}(\omega) = \hat{\varepsilon}(\omega) - i\,\frac{\kappa(\omega)}{\omega\varepsilon_o}; \quad \eta'(\omega) = \varepsilon'(\omega); \quad \eta''(\omega) = \varepsilon''(\omega) + \frac{\kappa}{\omega\varepsilon_o} \tag{6a,b,c}$$

Equation (5) may be used to replace κ in eqs.(6a,c) by the low frequency conductance of the sample measured at electrolyte concentration c.

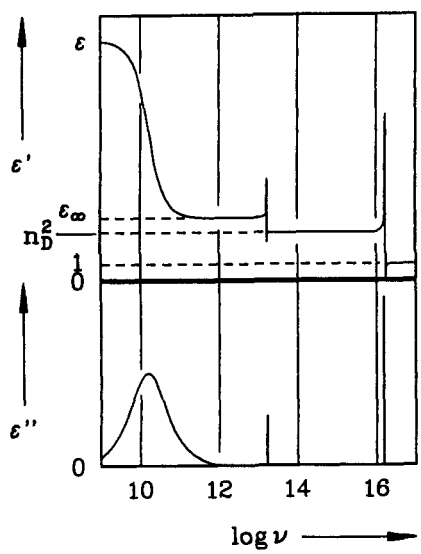

Fig. 1. Dielectric dispersion $\varepsilon'(\nu)$ and absorption $\varepsilon''(\nu)$ spectra for a polar liquid with a single Debye relaxation process in the microwave region and two resonant transitions in the IR and UV range; n_D is the refractive index in the visible spectral range.

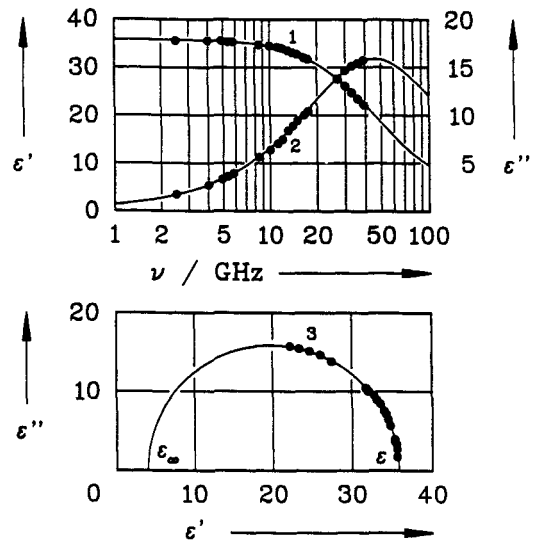

Fig. 2. Experimental data of acetonitrile at 25°C for $0.95 \leqq \nu/\mathrm{GHz} \leqq 40$ (•) and spectra calculated from the parameters of a Debye equation fitted to the data (Table 1) [48]. (1) dispersion ($\varepsilon'(\nu)$) and (2) absorption ($\varepsilon''(\nu)$) curve; (3) Argand diagram.

The dissipated energy per unit volume and time is

$$\dot{W} = \frac{1}{2}E_o^2\omega\varepsilon_o\eta'' \tag{7}$$

Theory of polarization shows that a periodically changing monochromatic electric field, $\vec{E}(t)=\vec{E}_o\exp(i\omega t)$, yields the frequency dependence of orientation polarization $\vec{P}_\mu(\omega,t)$ and induced polarization $\vec{P}_\alpha(\omega,t)$

$$\vec{P}_\mu(\omega,t) = \varepsilon_o(\varepsilon-\varepsilon_\infty)\,\vec{E}(t)\,\mathrm{L}_{i\omega}[f_P^{or}(t)]; \quad \vec{P}_\alpha(\omega,t) = \varepsilon_o(\varepsilon_\infty-1)\,\vec{E}(t) \tag{8a,b}$$

where $L_{i\omega}[f_P^{or}(t)]$ is the Laplace transform of the pulse response function $f_P^{or}(t)$

$$f_P^{or} = -\frac{\partial F_P^{or}}{\partial t}; \quad F_P^{or} = \frac{\langle \vec{P}_\mu(0) \cdot \vec{P}_\mu(t) \rangle}{\langle \vec{P}_\mu(0) \cdot \vec{P}_\mu(0) \rangle} \tag{9a,b}$$

The step response function of the sample, F_p^{or}, controls the restoration of the orientational contribution after a perturbation. For instance, if a constant electric field applied to a dipolar sample is switched off at time t=0, the orientational polarization monotonically decreases with time from $\vec{P}_\mu^{eq} = \vec{P}_\mu(0)$ to its final equilibrium value $\vec{P}_\mu(\infty)=0$ according to

$$\vec{P}_\mu(t) = \vec{P}_\mu^{eq} \cdot F_P^{or} \tag{10}$$

The step response function of reorientation is of relaxational type: $F_p^{or}(0)=1$; $F_p^{or}(\infty)=0$. Data analysis of microwave permittivity spectra begins with an assumption as to the type of the underlying step response function. If the polarization decay follows a first-order kinetic law, e.g. in the case of a single reorientation process

$$-\frac{d\vec{P}_\mu(t)}{dt} = k \cdot \vec{P}_\mu(t); \quad \vec{P}_\mu(t) = \vec{P}_\mu(0) \cdot \exp(-kt) \tag{11a,b}$$

it follows from a comparison of eqs.(10),(11) and (9) that

$$F_P^{or} = \exp\left(-\frac{t}{\tau}\right); \quad f_P^{or} = \frac{1}{\tau}\exp\left(-\frac{t}{\tau}\right); \quad L_{i\omega}[f_P^{or}] = (1+i\omega\tau)^{-1} \tag{12a,b,c}$$

The reciprocal rate constant k of the process is its relaxation time, $\tau=k^{-1}$. The combination of eqs.(8a) and (12c) yields the frequency dependence of permittivity for this process, called the "Debye relaxation process"

$$\hat{\varepsilon}(\omega) = \varepsilon_\infty + \frac{\varepsilon - \varepsilon_\infty}{1+i\omega\tau}; \quad \varepsilon'(\omega) = \varepsilon_\infty + \frac{\varepsilon - \varepsilon_\infty}{1+\omega^2\tau^2}; \quad \varepsilon''(\omega) = \frac{(\varepsilon - \varepsilon_\infty)\omega\tau}{1+\omega^2\tau^2} \tag{13a,b,c}$$

Figures 2 show the projections of the three dimensional curve $(\varepsilon',\varepsilon'',\nu)$ given by eq.(13a) in the (ε',ν)-plane (eq.(13b), dispersion curve (1)), in the (ε'',ν)-plane (eq.(13c), absorption curve (2)), and in the $(\varepsilon',\varepsilon'')$-plane (Argand diagram (3)) for the reorientation of acetonitrile in the frequency range from 0.95 to 40 GHz, where acetonitrile is one of the rare cases that follow a single Debye relaxation process, see Table 1. Figures 2 impart the knowledge of the relaxation parameters ε, ε_∞ from the Argand diagram, and τ, $\tau=1/\omega_{crit}$, from the maximum of the absorption curve or the inflection point of the dispersion curve. The quantity $\varepsilon_1-\varepsilon_\infty$ of the Argand diagram is called the dispersion amplitude of the relaxation process.

The first-order process shown in Fig.2 can be easily identified with the relaxation process in the microwave region of Fig.1. However, relaxation spectra are commonly more complex. Every molecular process changing the orientational polarization $\vec{P}_\mu$ of the sample, which can be understood as the vectorial sum of all dipole moments per unit of volume, causes a relaxation process of characteristic time constant τ_j (relaxation time).

PERMITTIVITY AND DIELECTRIC RELAXATION PARAMETERS OF PURE SOLVENTS

Table 1 gives a survey on relaxation parameters of selected solvents. Column 2 shows the static solvent permittivities ε_s determined at low frequencies ($\nu \leq 10$ MHz) with the usual equipment for this frequency range where no energy dissipation takes place, column 3 the range covered by the high frequency equipment and column 4 the assumption on the step function made for the data analysis for which the results are given in column 5a to 5i. Column 6 shows the square of the refractive index n_D^2 ($\varepsilon_D=n_D^2$) measured by optical methods (refractometry) at the wavelength of Na_D-line. Column 7 quotes the original literature. Columns 4 and 5a to 5i are explained in the following text.

Perusal of Table 1 shows that the representation of high frequency permittivity data with the help of a single Debye process (D_1 in Table 1) is only possible for limited frequency ranges and generally yields more or less correct data. To deal with the more complicated relaxation behaviour, usually detected with a broader frequency coverage, the analysis of the experimental data is based on a suite of distinct relaxation processes which may be Debye processes (D_1+D_2 and $D_1+D_2+D_3$ in Table 1) with discrete relaxation times or more or less broad relaxation time distributions around the relaxation time τ_j characterized by the parameters $\alpha_j > 0$ for symmetric and $\beta_j < 1$ for asymmetric distributions.

$$\hat{\varepsilon}(\omega) = \varepsilon_\infty + (\varepsilon - \varepsilon_\infty) \sum_{j=1}^{n} \frac{g_j}{[1+(i\omega\tau_j)^{1-\alpha_j}]^{\beta_j}} \tag{14a}$$

Equation (14a) contains Debye processes ($\alpha_j=0$, $\beta_j=1$), Cole-Cole processes ($0 \leq \alpha_j < 1$, $\beta_j=1$, CC in Table 1), and Cole-Davidson processes ($\alpha_j=0$, $0<\beta_j\leq 1$, CD in Table 1); n is the number of separable dispersion steps j of relaxation time τ_j, dispersion amplitude ($\varepsilon_j-\varepsilon_{\infty j}$) and weight

$$g_j = \frac{\varepsilon_j - \varepsilon_{\infty j}}{\varepsilon - \varepsilon_\infty}; \quad \varepsilon_{\infty j} = \varepsilon_{j+1}; \quad \varepsilon_1 = \varepsilon; \quad \varepsilon_{\infty n} = \varepsilon_\infty \tag{14b,c,d,e}$$

Table 1. Dielectric relaxation parameters of selected solvents at 25° C.

1		2	3	4	5a	5b	5c	5d	5e	5f	5g	5h	5i	6	7
compound		ε_s	$\frac{\nu_{min},\ \nu_{max}}{GHz}$	equation	ε	$\frac{\tau_1}{ps}$	α_1	β_1	$\varepsilon_2=\varepsilon_{\infty 1}$	$\frac{\tau_2}{ps}$	$\varepsilon_3=\varepsilon_{\infty 2}$	$\frac{\tau_3}{ps}$	$\varepsilon_{\infty 3}=\varepsilon_\infty$ resp. ε_∞	n_D^2	Ref.
water	H_2O	78.36	0, 60	D_1	78.36	8.27	0	1	5.16	—	—	—	5.16	1.7765	[5]
			0.9, 409	D_1+D_2	77.97	8.32	0	1	6.18	1.02	4.59	—	4.59		[3]
methanol	MeOH	32.63	0.9, 12	CC_1	32.64	50.2	0.014	1	5.27	—	—	—	5.27	1.7596	[6]
			0.9, 40	D_1+D_2	32.47	51.0	0	1	5.74	3.3	3.68	—	3.68		[7]
			0.9, 293	$D_1+D_2+D_3$	32.50	51.5	0	1	5.91	7.09	4.90	1.12	2.79		[3]
ethanol	EtOH	24.35	0.9, 89	$D_1+D_2+D_3$	24.32	163	0	1	4.49	8.97	3.82	1.81	2.69	1.8473	[3]
1-propanol	1-PrOH	20.439	0.9, 89	$D_1+D_2+D_3$	20.43	329	0	1	3.74	15.1	3.20	2.40	2.44	1.9146[a]	[3]
2-propanol	2-PrOH	19.385	0.9, 89	$D_1+D_2+D_3$	19.40	359	0	1	3.47	14.5	3.04	1.96	2.42	1.8912[a]	[3]
1-pentanol	1-PeOH	15.1[b]	0.01, 10	$D_1+D_2+D_3$	14.7	754	0	1	3.18	26	2.61	2.4	2.14	1.9824[a]	[9]
ethanediol*		40.8[c]	0.01, 70	D_1+D_2	42.8	145	0	1	7.3	10	3.8	—	3.8	2.0500[a]	[10]
1,2-propanediol*		32.0[a]	0.03, 10	D_1+D_2	29.2	430	0	1	5.9	40	3.9	—	3.9	2.0532[a]	[11]
formamide	FA	109.5	0.9, 89	CC_1+D_2	108.8	37.3	0.0057	1	7.08	1.16	4.48	—	4.48	2.096	[4]
N-methylformamide	NMF	185.98	0.9, 89	D_1+D_2	183.9	127	0	1	5.88	3.58	3.79	—	3.79	2.0449	[4]
			0.9, 293	$D_1+D_2+D_3$	183.3	128	0	1	6.13	7.93	4.60	0.78	3.20		
N,N-dimethylformamide	DMF	37.407	0.9, 293	D_1+D_2	37.24	10.4	0	1	4.38	0.76	2.94	—	2.94	2.0400	[4]
N,N-dimethylacetamide	DMA	38.60	0.9, 89	D_1+D_2	38.43	16.0	0	1	4.10	1.33	3.04	—	3.04	2.0618	[4]
tetramethylurea	TMU	23.5[c]	0, 0.25	D_1	—	31	0	1	—	—	—	—	—	2.100[a]	[14]
acetonitrile	AN	35.92	0.9, 40	D_1	35.77	3.48	0	1	4.00	—	—	—	4.00	1.7800	[4]
			0.9, 89	CC_1	35.96	3.21	0.028	1	2.26	—	—	—	2.26		
benzonitrile*	BN	25.2[c]	7.5, 38	D_1	25.6	38	0	1	3.9	—	—	—	3.9	2.328[a]	[15]
nitromethane		38.0[c]	1.9, 32	D_1	36	3.9	0.07	1	2	—	—	—	2	1.90[a]	[16]
propylene carbonate	PC	64.96	0.9, 89	CD_1	64.88	43.1	0	0.904	4.14	—	—	—	4.14	2.0153	[4]
dimethylsulfoxide	DMSO	46.48	0.9, 89	CD_1	46.40	20.5	0	0.888	4.16	—	—	—	4.16	2.1831[a]	[4]
acetone*	AC	20.56[c]	2.9, 24	D_1	21	3.3	0	1	2	—	—	—	2	1.84[a]	[17]
hexamethylphosphoric triamide	HMPA	29.6[c]	1.6, 12	D_1	29.6	80	0	0.92	3.3	—	—	—	3.3	2.1228[a]	[18]
pyrrolidone-(2)*		—	0.2, 36	D_1+D_2	28.8	253	0	1	11.7	19	5.8	—	5.8	2.214[a]	[19]
N-methylpyrrolidone-(2)*		—	0.02, 36	D_1	34.1	21	0	1	4.1	—	—	—	4.1	2.1228[a]	[19]
pyridine	Py	12.4[c]	0.9, 24	D_1	13.3	13.3	0	1	2.3	—	—	—	2.3	2.27[a]	[20]

* data at 20°C a) ref.[8] b) ref.[12] c) ref.[13]

Figure 3 shows an example where three Debye equations corresponding to three relaxation processes in the liquid must be assumed to reproduce the measured data.

Insufficient frequency coverage is responsible for many unsatisfactory data. On the other hand, an increase in the number of dispersion steps is not a sufficient criterion for the approach to the real relaxation behaviour of the sample. Strong support can be obtained from results of other methods probing dynamic properties, e.g. Rayleigh scattering, NMR relaxation or simulation studies; serious arguments for the assumption of dispersion steps result from examination of how the assumed relaxation processes of a solvent are influenced by the addition of electrolytes and non-electrolytes. A detailed discussion of the relaxation steps and their underlying processes of the solvents studied in our laboratory is given in refs. [2,3,4]. The intention of the actual paper is the provision of reliable, critically selected permittivity and dielectric relaxation data for the use of theoreticians and practising engineers. Suffice it therefore to give some brief information on the different relaxation processes in Table 1, which are arranged with regard to decreasing relaxation times. We prefer to assume a relaxation time distribution (CC or CD) if there are no convincing and verifiable arguments for a further splitting. At least for some systems where data had to be taken from the older literature (especially TMU), a more complex relaxation behaviour must be expected in an extended frequency range. A systematic study covering the region $0.95 \leq \nu/\mathrm{GHz} \leq 89$, of the dielectric properties of common solvents and their electrolyte solutions is in progress in our laboratory; this work will benefit from the construction of further equipment extending the accessible range to lower and higher frequencies in the near future.

For liquids of non-hydrogen-bonding molecules, one relaxation process can usually be found (often with a distribution of relaxation times, cf. Table 1) due to reorientation of the molecular dipoles. The processes at 1 ps for DMF and DMA (j=2) are due to hindered intramolecular reorientation around the C-N bond.

Hydrogen-bonding liquids show a more complex behaviour. The slow process characterized by τ_1 is cooperative in nature; the return of the bulk structure to equilibrium is accompanied by a marked change of the effective macroscopic dipole moment, leading to a large dispersion amplitude ($\varepsilon - \varepsilon_2$) of the mode. The fast process at relaxation times around 1 ps, numbered j=2 for water and formamide and j=3 for the monohydric alcohols and NMF, is connected with hydrogen-bond formation and decomposition

$$-\mathrm{H{:}X}- \rightleftharpoons -\mathrm{H} + {:}\mathrm{X}- \qquad (15)$$

The intermediate process (j=2) for the alcohols and NMF results from the reorientation of solvent molecules situated at ends of the hydrogen-bonded chains and/or monomers. This mode is not separable for the networks of water and FA [3,4].

From the above discussion it is evident that a broad frequency coverage is necessary to extract reliable information from complex permittivity spectra. To obtain the full information on the dynamics of the system, the inclusion of far-infrared data is desirable, although an upper frequency limit of about 100 GHz already gives satisfactory results in many cases. From our experience, we estimate that practically all liquids of medium to high polarity will exhibit a non-exponential relaxation behaviour with deviations from a single Debye equation well before the onset of librational modes.

The above considerations are of prime importance for theoretical and experimental investigations of the effect of solvent dynamics on chemical reactivity, a field which has attracted increasing interest in recent years. For an introduction the reader is referred to the reviews [21,22,23]. Implications in biochemistry are shown by Frauenfelder and Wolynes [24].

It has been shown [25] that the observed rate constants k_{obs} of electron transfer reactions can be conveniently expressed as

$$k_{obs} = K_p \kappa_{el} \nu_n \exp[-(\Delta G^*_{os} + \Delta G^*_{is}) / RT] \qquad (16)$$

where K_p is the equilibrium constant for the formation of the precursor state prior to electron transfer, κ_{el} is the electronic transmission coefficient, ν_n the nuclear frequency factor. ΔG^*_{os} and ΔG^*_{is} are the outer-shell (solvent) and inner-shell (bond distortion) activation barriers associated with the reaction. The influence of the solvent on the reaction rate emerges from the frequency factor ν_n and the outer-shell barrier ΔG^*_{os} both of which depend on the frequency dependent dielectric properties of the solvent.

For reactions with negligible ΔG^*_{is}, continuum theory, based on the assumption of a single Debye type relaxation process of time constant τ for the solvent, predicts ν_n to be proportional to the "longitudinal relaxation rate" τ_L^{-1}, $\tau_L \approx (\varepsilon_\infty/\varepsilon) \cdot \tau$ [26]. However, experimental results [27,28,29,30] do not corroborate this first-order approach, but imply a more complex behaviour with non-exponential solvent relaxation. This point is also stressed in the theoretical work of Hynes [31], who discusses the importance of the fast relaxation modes for the high rate constant k_{obs} observed in alcohols.

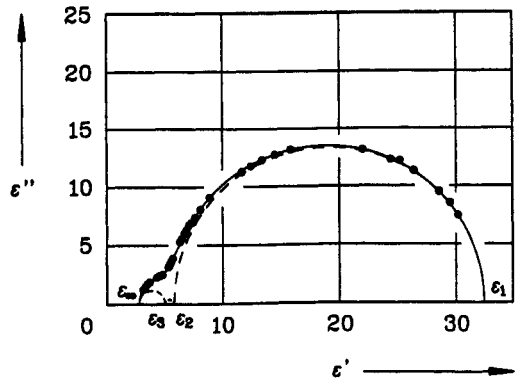

Fig. 3. Argand diagram calculated from a fit of three superimposed Debye equations (solid line) to experimental data (•) of methanol at 25°C for $0.95 \leq \nu/\mathrm{GHz} \leq 293$ [3]; far-infrared data are taken from [32]. The broken lines indicate the contributions of the individual relaxation processes with increasing relaxation time from left to right.

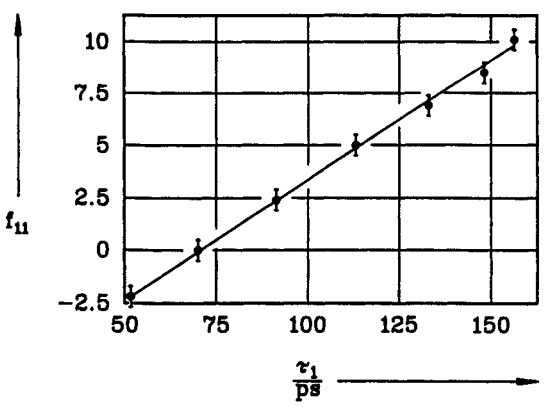

Fig. 4. Velocity correlation coefficients f_{11} of methanol/tetrachloromethane mixtures [39] as a function of the cooperative relaxation time τ_1 of the alcohol at 25° C [38].

PERMITTIVITY AND DIELECTRIC RELAXATION PARAMETERS OF NON-ELECTROLYTE SOLUTIONS

Investigation of the self- and hetero-association of molecules, i.e. the dielectric relaxation behaviour of apolar and polar solutes in hydrogen-bonding solvents, is another field which has attracted increased interest in the last few years. In this paper we shall confine our attention to the properties of solvent mixtures. For applications in the field of biophysics, the reader is referred to the monograph of Grant and coworkers [33] and to ref. [34] for more recent results.

For mixtures of 1-hexanol with n-heptane, a gradual decrease of the relaxation time of the cooperative process τ_1 is found and interpreted as gradual monomerization of the alcohol [35]. This is in contrast to results obtained for ethanol/cyclohexane systems [36], NMF/tetrachloromethane [37], and methanol/tetrachloromethane [2,38]. Here, the slow relaxation time of the polar component increases on initial dilution, pointing to a stabilization of the hydrogen-bonded entities by the added apolar component. For methanol/CCl_4 mixtures, a linear relation is found in the concentration range studied [38] (Fig.4) between τ_1, the cooperative relaxation of the hydrogen-bonded alcohol chains, and the velocity correlation coefficients of methanol f_{11}, obtained from self-diffusion coefficients [39]. This leads to the conclusion that self-association of the alcohol molecules dominates the dynamic behaviour of this system down to low methanol concentrations.

Systematic studies of n-alcohol/water mixtures have been performed by Gestblom and Sjöblom for alcohol-rich systems ($\leq$0.15 weight-% H_2O) at frequencies between 0.03 GHz and 10 GHz [40] and by Mashimo et al. [41] over the entire mixing range at $0.01 \leq \nu/\mathrm{GHz} \leq 15$. Both groups observed a marked decrease of τ_1, which is interpreted as a breaking up of the alcohol structure. This finding is corroborated by experiments up to 40 GHz with ethanol/water mixtures at the water-rich side [2], where a strongly reduced cooperative relaxation time of the alcohol τ'_1 is found; $\tau'_1 = \tau_1(2\varepsilon+\varepsilon_\infty)/(3\varepsilon)$ is the molecular or microscopic relaxation time with a minimum at 25 weight-% ethanol. Interestingly, τ'_2, the microscopic relaxation time attributed to water in the mixture shows a maximum at the same ethanol concentration, where the time constants τ'_1 and τ'_2 are practically equal, see Fig.5. This finding, together with thermodynamic data [42,43], indicates a high degree of interaction between water and alcohol in a structural arrangement with optimum space filling at this composition. It was found that the enthalpies, $\Delta_T H^\infty$, and entropies, $\Delta_T S^\infty$, for the transfer of KCl from water to ethanol/water mixtures are strongly influenced by the dielectric behaviour of the solvent [44].

Hydrophobic hydration is an important phenomenon in the understanding of water-organic molecule interaction and is investigated by dielectric spectroscopy. Kaatze and coworkers [45,46] have extensively studied aqueous solutions of substituted pyridines and related compounds. They found that both relaxation time and permittivity of the water in the hydration shell are increased when compared to the bulk solvent; this suggests a more ordered structure around the solute molecule. A clear distinction of the hydration shell permittivities of hydrophobic and hydrophilic ester surfaces was also found in kinetic investigations on ester solvolysis reactions [47].

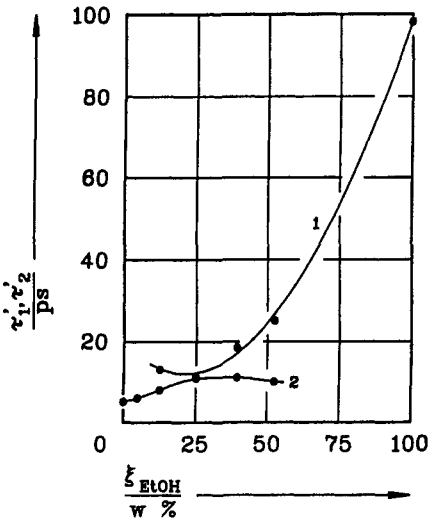

Fig. 5. Microscopic relaxation times in ethanol water mixtures as a function of alcohol weight fraction ξ_{EtOH} at 25°C [2]. 1: low frequency process of ethanol (τ'_1); 2: relaxation time of water (τ'_2).

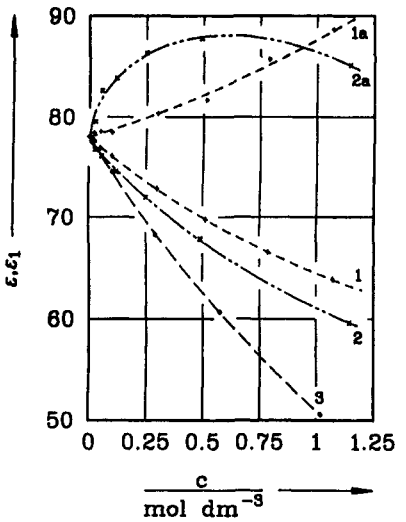

Fig. 6. Concentration dependence of the static permittivity of the solvent, ε_1, for aqueous solutions of $CdCl_2$ (curve 1), $CdSO_4$ (2), and $Cd(ClO_4)_2$ (3) at 25°C [38]. Curves 1a and 2a show the static permittivity of the electrolyte solution, ε, for $CdCl_2$ and $CdSO_4$ respectively; ε-ε_1 gives the contribution of the ion-pair relaxation process for these solutions.

PERMITTIVITY AND DIELECTRIC RELAXATION PARAMETERS OF ELECTROLYTE SOLUTIONS

The addition of electrolyte to a solvent yields three effects
- change in the dispersion amplitudes and relaxation times of the solvent relaxation processes
- appearance of a new relaxation region at the low frequency side of the $(\varepsilon', \varepsilon'', \omega)$-diagram whenever ion-pair relaxation of associating electrolytes occurs
- superposition of a contribution of electrolyte conductance, $\kappa/(\varepsilon_0\omega)$, which may be eliminated according to eq.(6) with the help of separately measured static conductances κ vs. c(ν<10 kHz; c: electrolyte concentration). In the following discussion, only conductance-corrected diagrams will be used. For complete diagrams including the conductance contributions, see ref. [48].

The bulk reorientation process of the solvent, j=1 in Table 1 is affected by a decrease of the solvent permittivity that is ion-specific and non-linear in electrolyte concentration

$$\varepsilon_1(c) = \varepsilon_1(0) - \delta_\varepsilon \cdot c + \beta_\varepsilon \cdot c^n \qquad (17)$$

with n=1.5 or n=2. The quantitiy δ_ε is called the dielectric decrement, $\delta_\varepsilon = \lim_{c\to 0}(-\partial\varepsilon_1/\partial c)$. As an example, Fig.6 shows the effect of cadmium salts on the permittivity of water, $\varepsilon_1(c)$ (curves 1-3). A marked difference is found for the concentration dependence of ε_1 of the 1:2-electrolytes $CdCl_2$ (curve 1) and $Cd(ClO_4)_2$ (curve 3) due to the effect of ion pairing detectable for the first system; the sulfate solutions (curve 2), where an ion-pair relaxation process is also found, show an intermediate behaviour. Figure 6 also shows the effect of the ion-pair relaxation process on the total permittivity ε of $CdCl_2$ (curve 1a) and $CdSO_4$ solutions (curve 2a). It either increases monotonously or exhibits a maximum in the concentration range studied.

A detailed discussion of the influence of ions on the solvent relaxation amplitude and relaxation times of various solvents is given in ref. [49]. Interestingly, positive and negative changes of the characteristic solvent relaxation time τ_1 are observed, depending on the nature of the ion-solvent interactions, but no influence of the ions can be detected on the relaxation time τ_3 (due to H-bonding) in the chain-forming solvents methanol and NMF.

The dielectric decrement is the central quantity in theories of irrotational bonding of the solvent molecules [51, 52] and of kinetic depolarization [53]. These theoretical concepts apply at the limit of infinite dilution, so that data of good quality at low electrolyte concentrations, rarely found in the literature, are needed to determine reliable values of δ_ε for the discussion. Table 2 gives a collection of coefficients determined from fits of $\varepsilon_1(c)$ in the concentra-

tion range $0 \leq c/\text{mol dm}^{-3} \leq c_{max}$ with $1\text{-}5 \cdot 10^{-2}$ mol dm^{-3} as the lowest electrolyte concentration investigated. For a discussion of irrotational bonding and related solvation numbers [52] and of kinetic depolarization [53], the reader is referred to [49] and the literature quoted therein.

Table 2. Coefficients of eq.(17) for the static permittivity of the solvent in electrolyte solutions, $\varepsilon_1(c)$, at 25°C

solvent	electrolyte	δ_ε / dm^{3}mol^{-1}	β_ε / (dm^{3}mol^{-1})^n	n	c_{max} / mol dm^{-3}
water	Na_2SO_4	30±2	10±2	1.5	1.0
	$MgCl_2$	34±1	10±1		1.0
	$MgSO_4$	32±1	13±1		1.1
	$CdCl_2$	22.4±0.3	8.9±0.2		1.5
	$Cd(ClO_4)_2$	39.8±0.7	12.8±0.7		1.0
	$CdSO_4$	28±2	12±2		1.1
	$CuCl_2$	39±2	17±2		1.1
methanol	NaCl	56±5	66±13	1.5	0.14
	NaBr	42±2	26±3		0.7
	NaI	39±2	21±2		1.0
	$NaClO_4$	33±1	19±1		1.1
	NH_4Br	33±4	17±4		0.8
	Bu_4NCl	42±1	24±1		0.8
	Bu_4NBr	41±6	26±8		0.5
	Bu_4NI	30±2	18±2		0.8
	Bu_4NClO_4	21±2	10±2		0.8
acetonitrile	LiBr	5.35±0.05	—	0	0.7
	NaI	7.5±0.8	3.1±0.9	2	0.9
	$NaClO_4$	8.0±0.3	2.1±0.2		1.9
	Bu_4NBr	13.7±0.2	2.4±0.1		1.4
formamide	$NaClO_4$	29±1	4.9±1.4	2	0.9
NMF	$NaClO_4$	155±3	61±4	2	0.9
DMF	$NaClO_4$	17.0±0.8	4.2±0.8	2	1.0
DMSO	LiNCS	20.0±0.6	7.8±0.5	1.5	1.6

Table 3. Association constants of ion-pair formation from dielectric relaxation data (K_A) and literature values $K_A^{Lit.}$ at 25° C

solvent	electrolyte	IP	K_A / dm^3 mol^{-1}	K_A^{Lit} / dm^3 mol^{-1}
water	Na_2SO_4	SSIP	18±1	4.5[65]
	$MgSO_4$	SSIP	164±25	174[64]
	$CdCl_2$	CIP	105±65	85[66]
	$CdSO_4$	SSIP	270±90	245[62]
methanol	Bu_4NClO_4	CIP	44±17	47.1[67]
acetonitrile	LiBr	CIP	148±2	155—193*
	NaI	CIP	17±6	3.8—24*
	$NaClO_4$	CIP	31±3	15—27*
	Bu_4NBr	CIP	17±1	17—22*
DMF	$NaClO_4$	SSIP	1.9±1.3	3.2±0.7[68]
DMSO	LiNCS	CIP	≈ 3	≈ 1[69]

* re-analysis of conductance data from the literature

An important application of concentration-dependent solvent permittivities, eq.(17), is their use in the calculation of thermodynamic properties of electrolyte solutions with the help of "effective interaction potentials" [54,55,56,57] instead of mean force potentials at infinite dilution used at the McMillan-Meyer (MM) level. MM models imply the use of the permittivity of the pure solvent in the ion-ion interactions up to high electrolyte concentrations, in contrast to effective interaction models which use solvent permittivities $\varepsilon_1(c)$ depending on electrolyte concentration.

Effective interaction models based on some extension of the Debye-Hückel theory were applied in refs.[58,59]. HNC-calculations of the osmotic coefficient for methanol solutions of tetraalkylammonium and sodium salts are reported in ref.[60]. An example, Figure 7, comparing the results from HNC calculations at MM-level and effective interaction potential level with measured osmotic coefficients, illustrates the role of solute concentration dependent permittivities. Unfortunately, the full set of data (vapour pressure, solvent compressibility, permittivity) needed for a study of the influence of the concentration-dependent solvent permittivity on HNC calculations of osmotic coefficients is only available for very few systems at present.

ION EQUILIBRIA IN ELECTROLYTE SOLUTIONS

Formation of neutral ion-pair dipoles gives rise to additional relaxation processes on the low frequency side of the dispersion, absorption and Argand diagrams. This feature is documented by many publications [51,6,52]. In preceding papers [62,63], we have shown that the dispersion amplitudes of the ion-pair relaxation process yield association constants in agreement with those obtained by classical methods such as molar conductance, e.m.f., heat of dilution or vapour pressure measurements, cf. Table 3, and also permit the identification of the type of ion pair in the solution. Table 3 compares association constants K_A determined from ion-pair dispersion amplitudes with selected literature data $K_A^{Lit.}$, mostly from conductance studies. The third column of Table 3 informs on the type of ion pair dominating in the solution. Here CIP stands for contact ion pair, SSIP for solvent-shared ion pair. A commonly observed concentration dependence of the ion-pair relaxation time is explained by the superposition of two modes, the reorientation of the ion-pair dipole in the electric field (diffusive rotational motion) and the formation and decomposition of the ion pair (kinetic mode) [7], permitting the determination of very fast rate constants of ion-pair formation (up to $k \approx 5 \cdot 10^9$ dm^{3}mol^{-1}s^{-1}) and dissociation (up to $k \approx 2 \cdot 10^9$ s^{-1}) [49].

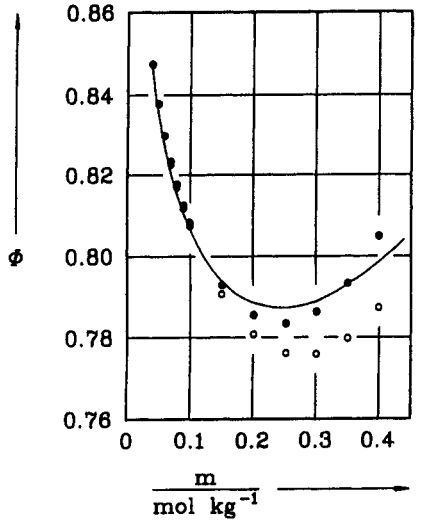

Fig. 7. Osmotic coeffcients ϕ for Bu_4NBr in methanol [60]. Experimental curve (—) and results from HNC calculations at McMillan-Mayer (o) and effective interaction potential level (•).

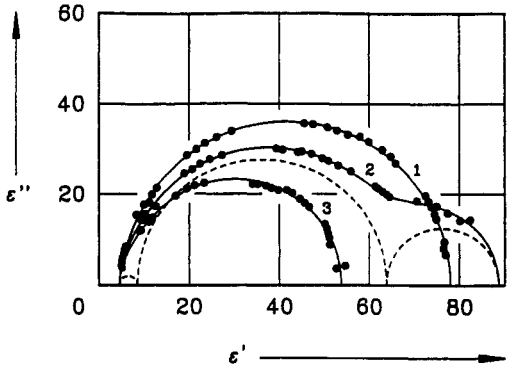

Fig. 8. Argand diagrams of water (curve 1, far-infrared data taken from ref. [50] and aqueous solutions of 1.07 mol dm^{-3} $CdCl_2$ (2) and 0.98 mol dm^{-3} $MdCl_2$ (3) at 25° C [38]. The broken lines indicate (from right to left) the individual contributions of the ion pair, the cooperative processes (τ_1, cf. Table 1) and the high frequency process (τ_2) of water to the total dispersion given by curve 2.

Recent extension of these investigations to the formation of charged ion-pair species such as $[NaSO_4]^-$ or $[CdCl]^+$ open the field of complex formation studies for microwave permittivity investigations. Figure 8 shows Argand diagrams of pure water and almost equally concentrated solutions of $MgCl_2$ and $CdCl_2$, from which it follows that $MgCl_2$ does not form ion pairs in contrast to $CdCl_2$ for which the dispersion amplitude indicates strong association to $[CdCl]^+$; higher aggregates such as $[CdCl_3]^-$ should have little influence on the spectra in the frequency range studied.

CONCLUSION

Dielectric relaxation studies have proved to be an efficient tool for the study of molecular processes in solutions when carried out over sufficiently large frequency ranges. Important information, not accessible by other techniques, can be obtained and used to explain solvent and solution properties, or to calculate properties of mixtures and solutions in the framework of molecular theories.

Acknowledgement

We are grateful to the Deutsche Forschungsgemeinschaft for the generous support of our investigations.

REFERENCES

1. C.F.J. Böttcher and P. Bordewijk, Theory of Electric Polarization 2, (2nd ed.), Elsevier, Amsterdam (1978).
2. J. Barthel, R. Buchner, and H. Steger, Wiss. Zeitschr. THLM 31, 409-423 (1989).
3. J. Barthel, K. Bachhuber, R. Buchner, and H. Hetzenauer, Chem.Phys.Lett. 165, 369-373 (1990).
4. J. Barthel, K. Bachhuber, R. Buchner, B. Gill, and M. Kleebauer, Chem.Phys.Lett. 167, 62-66 (1990).
5. U. Kaatze and V. Uhlendorf, Z.Phys.Chem.NF 126, 151-156 (1981).
6. B. Kaukal, PhD-Thesis, Regensburg (1982).
7. J. Barthel, K. Bachhuber, and R. Buchner, in: M. Moreau and P. Turq (eds.), Chemical Reactivity in Liquids - Fundamental Aspects, Plenum Press, New York, 55-71 (1989).
8. J.A.Riddick, W.B. Bunger, and T.K. Sakano, in: A. Weissberger (ed.), Techniques of Chemistry 2 (4th ed.), Wiley, New York (1986).
9. Y. Dutuit, J.S. Salefran, A.M. Bottreau, R. Cahine, and T.K. Bose, Adv.Mol.Relax.Proc. 23, 75-95 (1982).
10. B.P.Jordan, R.J. Sheppard, S. Szwarnowski, J.Phys.D: Appl.Phys. 11, 695-701 (1978).
11. A. El-Samahy, B. Gestblom, and J. Sjöblom, Finn.Chem.Lett. 54-58 (1984).
12. A. D'Aprano, I.D. Donato, G. D'Arrigio, D. Bertolini, M. Cassetari, and G.Salvetti, Mol. Phys. 55, 475-488 (1985).

13. J. Barthel, H.J. Gores, G. Schmeer, and R. Wachter, in: F.L. Boschke (ed.), Topics in Current Chemistry 111, 35-144 (1983).
14. T. Gäumann, Helv.Chim. Acta 41, 1956-1970 (1958).
15. J.P. Poley, Appl.Sci.Res. B4, 337-387 (1955).
16. S. Chandra and D. Nath, J.Chem.Phys. 51, 5299-5304 (1969).
17. J.H. Calderwood and C.P. Smyth, J.Am.Chem.Soc. 78, 1295-1297 (1956).
18. H. Behret, F. Schmithals, and J. Barthel, Z.Phys.Chem.NF 96, 73-88 (1975).
19. E. Dachwitz and M. Stockhausen, Ber. Bunsenges. Phys. Chem. 89, 959-961 (1985).
20. R.S. Holland and C.P. Smyth, J.Phys.Chem. 59, 1088-1092 (1955).
21. J.D. Simon, Accounts Chem.Res. 21, 128-134 (1988).
22. B. Bagchi, Annu.Rev.Phys.Chem. 40, 115-141 (1989).
23. B. Bagchi and G.R. Fleming, J.Phys.Chem. 94, 9-20 (1990).
24. H. Frauenfelder and P.G. Wolynes, Science 229, 337-345 (1985).
25. J.T. Hupp and M.J. Weaver, J.Electroanal.Chem. 152, 1-14 (1983).
26. D.F.Calef and P.G. Wolynes, J.Chem.Phys. 78, 4145-4153 (1983).
27. M. Marconelli, E.W. Castner Jr., B. Bagchi, and G.R. Fleming, Faraday Discussions Chem.Soc. 85, 199-210 (1988).
28. R.M. Nielson, G.E. McManis, M.N. Golovin, and M.J. Weaver, J.Phys.Chem. 90, 3441-3450 (1988).
29. M.J. Weaver, G.E. McManis, W. Jarzeba, and P.F. Barbara, J.Phys.Chem. 94, 1715-1719 (1990).
30. G. Grampp, A. Kapturkiewicz, and W. Jaenicke, Ber. Bunsenges. Phys. Chem. 94, 439-447 (1990).
31. J.T. Hynes, J.Phys.Chem 90, 3701-3706 (1986).
32. R. Buchner and J. Yarwood, Mikrochim.Acta 2, 335-337 (1988).
33. E.H. Grant, R.J. Sheppard, and G.P. South, Dielectric Behaviour of Biological Molecules in Solution, Oxford University Press (Clarendon), London (1978).
34. S. Mashimo, S. Kuwabara, S. Yagihara, and K. Higasi, J.Phys.Chem. 91, 6337-6338 (1987).
35. E. Noreland, B. Gestblom, and J. Sjöblom, J. Solution Chem. 18, 303-312 (1989).
36. M.W. Sagal, J.Chem.Phys. 36, 2437-2442 (1962).
37. R. Groot-Wassink and P. Bordewijk, Adv.Mol.Relax.Proc. 13, 299-308 (1978).
38. unpublished results from the authors' laboratory
39. S. Prabhakar and H. Weingärtner, Z.Phys.Chem.NF 137, 1-12 (1982).
40. B. Gestblom and J.Sjöblom, Act.Chem.Scand. A38, 47-56 and 575-578(1984).
41. S. Mashimo,S. Kuwabara, S. Yagihara, and K.Higasi, J.Chem.Phys. 90, 3292-3294 (1989).
42. J.A. Larkin, Chem.Thermodyn. 7, 137-148 (1975).
43. S.K. Maity, A.K. Chattopadyad, and S.C. Lahiri, Electrochim.Acta 25, 1487-1490 (1980).
44. J. Barthel, H. Steger, and J. Wölbl, unpublished results.
45. U. Kaatze, C. Neumann, and R. Pottel, J. Solution Chem. 16, 191-204 (1987).
46. U. Kaatze, R. Pottel, and P. Schmidt, J.Phys.Chem. 92, 3669-3674 (1988).
47. G. Schmeer and J. Barthel, J.Solution Chem., in press.
48. J. Barthel and M. Kleebauer, J.Solution Chem., in press.
49. J. Barthel, R. Buchner, K. Bachhuber, H. Hetzenauer, M. Kleebauer, and H. Ortmaier, Pure Appl.Chem., in press.
50. J.B. Hasted, S.K. Husain, F.A.M. Frescura, and J.R. Birch, Infrared Phys. 27 11-15 (1987).
51. U. Kaatze, Z.Phys.Chem.NF 135, 51-75 (1983).
52. J.-P. Badiali, H. Cachet, and J.C. Lestrade, Pure Appl.Chem. 53 1383-1399 (1981).
53. J.B. Hubbard, P. Colonomos, and P.G. Wolynes, J.Chem.Phys. 71, 2652-2661 (1979).
54. S.A. Adelman, J.Chem.Phys. 64, 724-731 (1976).
55. S.A. Adelman, Chem.Phys.Lett. 38, 567-570 (1976).
56. H.L. Friedman, J.Chem.Phys. 76, 1092-1105 (1982).
57. P.G. Kusalik and G.N. Patey, J.Chem.Phys. 79, 4468-4474 (1983).
58. J. Barthel, J.Chim.Phys.Special Issue October 1969, 199-203 (1969).
59. J.C.Martin, J.L. Gomez-Estévez, and M. Canales,J.Solution Chem. 16, 87-104 (1987).
60. W. Kunz and J. Barthel, J. Solution Chem. 19, 339-352 (1990).
61. U. Kaatze, V. Lönnecke, and R.Pottel, J.Phys.Chem. 91, 2206-2211 (1987).
62. J. Barthel, R. Buchner, and H.-J. Wittmann, Z.Phys.Chem.NF 139, 23-37 (1984).
63. J. Barthel and R. Buchner, Pure Appl.Chem. 58, 1077-1090 (1986).
64. H.-J. Wittmann, PhD-Thesis, Regensburg (1985).
65. R.M. Izatt, D. Eatough, J.J. Christensen, and C.H. Bartholomew,J.Chem.Soc. A 47-53 (1969).
66. P.J. Reilly and R.H. Stokes, Aust.J.Chem. 23, 1397-1402 (1970).
67. J. Barthel, M. Krell, L. Iberl, and F. Feuerlein, J. Electroanal.Chem. 214, 485-505 (1986).
68. B.S. Krumgalz and J. Barthel, Z.Phys.Chem.NF 142, 167-178 (1984).
69. J.B. Gill and P. Longdon, unpublished results.